Excitonic effects in the photoinduced conduction intersubband transitions in undoped quantum wells

S. M. Sadeghi*
Department of Physics, University of Toronto, 60 St. George Street, Toronto, Canada M5S 1A7

W. Li
Department of Chemical and Engineering Physics, University of Wisconsin–Platteville, Platteville, Wisconsin 53818, USA
(Received 17 April 2004; revised manuscript received 16 August 2004; published 16 November 2004)

We study the effects of excitons and their optical excitation or radiative decay in the photoinduced conduction intersubband transitions of undoped quantum wells. We show that the excitonic effects, in general, can strongly influence these transitions by making their dipole moments strongly dependent on the hole subband dispersions and quantum well strain. This allows spinor mixing of a hole subband to significantly suppress a photoinduced intersubband transition when this subband is strongly nonparabolic and/or is about to crossover another subband. Compared to those happening in the absence of any interband transition, however, we show that when the photoinduced intersubband transitions are accompanied with the optical excitation or radiative decay of excitons (excitonic interband transitions) their electric dipole moments can suffer an additional suppression. We attribute this effect to the influence of the correlation between the electron and hole positions in the photoinduced intersubband transitions and the way it depends on the excitonic interband transitions. In all cases, however, our results suggest that ignoring the effects of excitons in the conduction intersubband transitions of undoped quantum wells, i.e., considering only electron wave functions, could lead to an unrealistic overestimation of their dipole moments.

DOI: 10.1103/PhysRevB.70.195321 PACS number(s): 78.67.De, 78.66.Fd

I. INTRODUCTION

Intersubband transitions (IST) between quantized levels of low-dimensional quantum structures are useful tools for study of fundamental properties of semiconductors and development of optical devices. In quantum well (QW) structures these transitions were used to design modulators,[1] photodetectors,[2] and lasers,[3] and to investigate various aspects of physics of semiconductors.[4,5] Recently these transitions were also used to study quantized states of quantum dots[6] and quantum wires.[7] Many of these studies have been reported for undoped QW structures where infrared (IR) laser beams near resonant with the transitions between the confined states of the conduction band were employed to investigate their energies, relaxation times, etc. Since these transitions occur in the presence of laser fields responsible for the interband excitation of electrons, they are usually called photoinduced intersubband transitions (PI IST).

Due to the fact that the PI ISTs occur in the presence of the photo-excited holes generated simultaneously by the interband laser fields, they can be distinctively different from those happening in n-doped QWs. Although this issue plays an important role in the study of nonlinear optical processes in QWs and design of optical devices, the results of the previous studies are rather contradictory. For example, while in Ref. 8 the experimental results were interpreted as a sign of enhancement of the oscillator strengths of PI ISTs via Coulomb interaction between electrons and holes (excitonic effects), in Ref. 9 no enhancement was inferred from the experimental results. Therefore, in contrast to the former, the latter dismissed any effect due to the Coulomb interaction and concluded that the PI ISTs in undoped QWs were basically similar to those in n-doped QWs. Recently, however, we showed that depending on the hole dispersions, the Coulomb interaction between photoexcited electrons and holes can play a crucial role in the PI ISTs.[10] Our results showed that due to the excitonic effects caused by such interaction the dipole moments of these transitions were influenced by the spinor mixing of the valence subbands. It was shown that in an undoped QW structure containing only two conduction subbands this effect could lead to multi-level mixing of the exciton states, although the structure was interacting with a single IR field near resonance with the transitions between these subbands.[10] Under no conditions, however, the excitonic nature of the PI IST was found to enhance the dipole moments of these transitions.

An important feature of the PI ISTs is that although they happen as electrons are optically excited from one conduction subband ($e1$) to another ($e2$), they are in fact transitions between the exciton states associated with these subbands (see Fig. 1). Therefore, these transitions can occur while the excitons associated with e1 ($e1$-$hh1$ or $e1$-$lh1$) are being optically generated or decaying radiatively (active excitons), or they are in their nonradiative states or in their life spans (nonactive excitons). The former (active excitons) refers to the case where the PI ISTs are accompanied with the excitonic interband transitions [Fig. 1(b)]. Examples for this case include the PI ISTs associated with the optical quantum confined Stark effects where an intense IR laser beam resonant with the e1-e2 transition was used to modify the interband excitonic absorption,[11] or emission.[12] The PI ISTs associated with the nonactive excitons, however, are characterized by the absence of any excitonic interband transition [Fig. 1(c)]. Such PI ISTs can happen when the momenta of the e1-hh1 or e1-lh1 excitons (K) are larger than those of the photons ($q \sim 0$) responsible for the excitation of the electron-hole

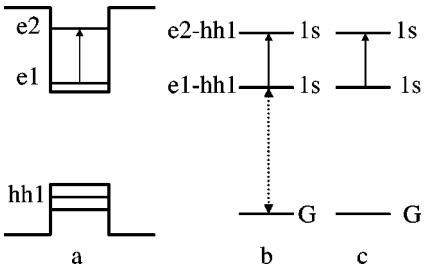

FIG. 1. (a) Schematic illustration of the square QW structures considered in this paper; (b) and (c) represent the PI ISTs associated with the excitons in the presence and absence of excitonic interband transitions, respectively. The one-sided arrows refer to the ISTs and the two-sided one to the optical excitation or radiative decay processes of the excitons.

pairs.[13,14] They can also occur effectively when the electron-hole pairs are widely separated and the exciton lifetime is prolonged. This situation can happen, for example, in a double QW structure where electrons and holes are kept in two different wells separated by a barrier.[15]

In this paper we theoretically study the distinctive features of the PI ISTs associated with the active and nonactive excitons including the effects of strain and QW thickness. Our results show that similar to those associated with the nonactive excitons, when the PI ISTs are accompanied with the excitonic interband transitions (active excitons) their dipole moments depend strongly on the spinor mixing and dispersions of the hole subbands. This causes immense suppression of these moments when these subbands are significantly nonparabolic and/or because of strain they are about to crossover one another. The dipole moments associated with the active excitons, however, suffer an additional suppression, depending on the thickness of the QW structure and strain. In narrow QWs such a suppression can be drastic while in wide QWs under extensive compressive strain it becomes insignificant. We attribute these effects to the convolution of the conduction intersubband transitions with the hole probability. Such a convolution, which does not exist in the case of the PI ISTs associated with the nonactive excitons, is originated from the correlation between electron and hole coordinates as the excitonic interband transitions happen.

Note that in many nano-structures the effects of strain are dramatic. Therefore, the results of this paper can shed some light on the investigations of the optical processes in such structures where the PI ISTs are used to understand their energy states or relaxation mechanisms[6,7] or to alter their optical responses. In addition, these results can also provide a realistic evaluation of the dipole moments of the PI ISTs used to probe time evolution of excitons or photo-excited electrons,[4,16] or to generate quantum interference effects when they are accompanied with the interband transitions.[17] Moreover, when accompanied with the possibility of multilevel mixing of excitons,[10] they can be useful in the studies where strong IR or Terahertz (THz) fields are used to drive the PI ISTs and to dress the exciton states.[18–20] This issue is particularly important when one deals with the design of optical devices such as all-optical modulators that are based on PI ISTs.[21,22]

II. EXCITONIC EFFECTS IN THE PHOTOINDUCED INTERSUBBAND TRANSITIONS IN UNDOPED QUANTUM WELLS

As mentioned in the introduction, a key feature for the treatment of the PI ISTs between the conduction subbands of an undoped QW is inclusion of Coulomb interaction between electrons in these subbands and holes in the valence band. In the limit of low carrier excitation and low excess kinetic energies such Coulomb interaction create excitons. Because of the PI ISTs, these excitons are associated with the electrons in the ground conduction subband (e1) and the upper one(s) (e2). In general the states of these excitons can have different orbital angular momenta (s,p states, etc.) and principal quantum numbers. They can also be involved with several valence subbands, representing states with mixture of orbital angular momenta. In the following for the sake of simplicity we ignore the Coulomb mixing between the hole subbands that is responsible for such an angular momentum mixing. This is because we do not expect these effects to be significant and, as will be discussed in the following, their inclusion does not change the physical processes discussed in this paper. Under such conditions one can construct the states of the excitons from the electron ($|\mathbf{k},i\rangle$) and hole states ($|\mathbf{k},j\rangle$) as follows:

$$\Psi_{ij}^{\xi,\beta} = \sum_{\mathbf{k},\mathbf{k}'} M_{i,j}^{\xi,\beta}(\mathbf{k},\mathbf{k}')|\mathbf{k},i\rangle|\mathbf{k}',j\rangle. \tag{1}$$

Here i and j refer to the electron and hole subband indices, respectively. In this paper since we consider QW structures that only support two conduction subbands, we have i=e1 and e2. Moreover, we only consider the first heavy and light hole subbands, i.e., j=hh1 and lh1. ξ and β in Eq. (1) refer to the total angular momentum and energy index of an exciton ($\beta=1s,2s,2p$, etc.), respectively. For excitons with zero momenta ($\mathbf{K}=0$), the envelop function $M_{i,j}^{\xi,\beta}(\mathbf{k},\mathbf{k}')$ is given by

$$M_{i,j}^{\xi,\beta}(\mathbf{k},\mathbf{k}') = \delta(\mathbf{k}+\mathbf{k}')G_{i,j}^{\xi,\beta}(\mathbf{k}). \tag{2}$$

The exciton relative envelope function, $G_{i,j}^{\xi,\beta}(\mathbf{k})$, is governed by the following equation:

$$[E^c(i,k)+E^h(j,k)]G_{i,j}^{\xi,\beta}(\mathbf{k}) + \sum_{\mathbf{q}\neq 0} V_{ij}(q)G_{i,j}^{\xi,\beta}(\mathbf{k}+\mathbf{q}) = E_{i,j}^{\xi,\beta}G_{i,j}^{\xi,\beta}(\mathbf{k}). \tag{3}$$

Here $E_{i,j}^{\xi,\beta}$ are the transition energies of the excitons and $V_{ij}(q)$ refers to the Coulomb interaction between the electrons and holes. The states of these electrons and holes are given by:

$$|\mathbf{k},i\rangle = e^{i\mathbf{k}\cdot\rho_\mathbf{e}}C_i(z)U_0(\mathbf{r}_\mathbf{e}), \tag{4}$$

$$|\mathbf{k},j\rangle = e^{i\mathbf{k}\cdot\rho_\mathbf{h}}\sum_\nu v_{j,\mathbf{k}}^\nu(z)U_0^\nu(\mathbf{r}_\mathbf{h}). \tag{5}$$

Here $\rho_\mathbf{e}$ and $\rho_\mathbf{h}$ refer to the in-plane coordinates of an electron and hole with the Bloch functions represented by U_0 and U_0^ν, respectively. C_i represents the envelope function of electrons in the ith conduction subband with energy $E^c(i,k)$. $v_{j,\mathbf{k}}^\nu(z_h)$ refers to the envelope function of a hole in the jth

subband (hh1 and lh1) with energy $E^h(j,k)$. ν is the spinor of the holes taking $\pm 3/2$ for heavy holes and $\mp 1/2$ for light holes. In this paper we obtain the hole envelope functions using the $\mathbf{k}.\mathbf{p}$ method and solving a 4×4 Luttinger-Kohn Hamiltonian. In the following, for the sake of simplicity, we only consider $\nu=3/2$ for the heavy holes and $\nu=-1/2$ for the light holes.

In practice, to induce the PI ISTs in undoped QWs one needs an interband laser field to resonantly or near resonantly create excitons while at the same time an IR field excites electrons from one conduction subbands to another. In general the dipole moments of such PI ISTs can be given by:

$$\mu_{ii'j}^{\xi,\beta}=\sum_{\nu}\mu_{ii'j}^{\xi\nu\beta}, \tag{6}$$

where

$$\mu_{ii'j}^{\xi\nu\beta}=\langle F_{ij}^{\xi\nu\beta}|z_e|F_{i'j}^{\xi\nu\beta}\rangle. \tag{7}$$

Here $F_{ii'j}^{\xi\nu\beta}$ refer to the envelop functions of the exciton states associated with the initial and final states of these transitions. They are given by:[23]

$$F_{ij}^{\xi\nu\beta}=\frac{1}{(2\pi)^{3/2}}\int d\mathbf{k}G_{i,j}^{\xi,\beta}(\mathbf{k})e^{i\mathbf{k}.(\rho_{\mathbf{e}}-\rho_{\mathbf{h}})}C_i(z_e)v_{j,\mathbf{k}}^{\nu}(z_h). \tag{8}$$

The sum over ν in Eq. (6) emphasizes on the fact that generally various hole spinors can contribute to the dipole moments of the PI ISTs. This is associated with the fact that the states of excitons can contain various components associated with these spinors. However, due to the interband selection rules, in narrow QWs mostly the *s* state excitons are excited. This limits $\nu=+3/2$ for the e1-hh1 exciton, and $\nu=-1/2$ for the e1-lh1 exciton. Therefore, for such cases one can drop the index ν in Eq. (6) or just use Eq. (7). Note that even in the presence of the Coulomb hole subband mixing effects where the exciton states can become mixtures of heavy-hole and light-hole spinors,[24] the treatment presented in this paper remains valid. Under this condition, however, in addition to the transitions between the 1*s* states of the excitons associated with e1 and e2, those between exciton states with different orbital angular momenta (p,d, etc.) should also be included. This requires not only the sum over ν in Eq. (6), but also addition of a sum over j. Note that even in such cases the contributions of the 1s states usually remain the most significant one.[25] Therefore, for the sake of simplicity, in the following we only consider the PI ISTs that occur between the 1*s* states of the e1-hh1 and e2-hh1 excitons [Figs. 1(b) and 1(c)] and between the 1s states of the e1-lh1 and e2-lh1 excitons. Under these conditions we have $\beta=1s$, $\xi=\nu=3/2$ for e1-hh1 or e2-hh1, and $\xi=\nu=-1/2$ for e1-lh1 or e2-lh1.[23] For this reason in the following we drop the ξ and β (or 1s) indices for simplicity. Note also that in Eqs. (7) and (8) we applied the selection rules of the PI ISTs that only allow transitions between exciton states with the same total and orbital angular momenta.

The main distinctive feature of the PI ISTs associated with the active excitons is that they occur in the presence of the interband transitions, such as absorption or emission of excitons. As a result, they happen under the condition of zero distance between the electrons and holes. Considering this and introducing μ_j^{act} to represent Eq. (7) under such a condition, we find:

$$\mu_j^{\mathrm{act}}=\mathrm{L}\int \mathrm{kdk}g_{\mathrm{e1},j}(\mathrm{k})g_{\mathrm{e2},j}(\mathrm{k})I_{1,j}^{\nu}(\mathrm{k}), \tag{9}$$

where

$$I_{1,j}^{\nu}(\mathrm{k})=\int zdzC_{\mathrm{e1}}(z)C_{\mathrm{e2}}^{*}(z)|v_{j,\mathrm{k}}^{\nu}(z)|^2. \tag{10}$$

To obtain Eqs. (9) and (10) we applied the following equations:[23]

$$G_{i,j}^{\xi,\beta}(\mathbf{k})=e^{j\xi\alpha}g_{i,j}^{\xi,\beta}(\mathrm{k}) \tag{11}$$

and

$$v_{j,\mathbf{k}}^{\nu}(z_h)=e^{-j\nu\alpha}v_{j,\mathrm{k}}^{\nu}(z_h), \tag{12}$$

where $\mathbf{k}\equiv(\mathrm{k},\alpha)$.

When the e1-hh1 or e1-lh1 excitons are not decaying or optically excited (nonactive excitons) the condition of the zero distance between electron and hole coordinates is not applied. Representing Eq. (7) for such a case with μ_j^{nact}, here we find that the dipole moments of the PI IST associated with these excitons as follows:

$$\mu_j^{\mathrm{nact}}=\mu_{12}^{\mathrm{ele}}\int \mathrm{kdk}g_{\mathrm{e1},j}(\mathrm{k})g_{\mathrm{e2},j}(\mathrm{k})I_{2,j}^{\nu}(\mathrm{k}), \tag{13}$$

where

$$\mu_{12}^{\mathrm{ele}}=\int dz_eC_{\mathrm{e1}}^{*}(z_e)z_eC_{\mathrm{e2}}(z_e) \tag{14}$$

and

$$I_{2,j}^{\nu}(\mathrm{k})=\int dz_h|v_{j,\mathrm{k}}^{\nu}(z_h)|^2. \tag{15}$$

Here μ_{12}^{ele} refers to the electric dipole moment of the transition between e1 and e2 excluding any excitonic effect, i.e., only conduction subband wavefunctions are included. Note that Eqs. (13)–(15) bear the approximation that nonactive exciton states have envelop functions similar to those of radiative excitons. In fact here we use hydrogen-like wave functions for the 1*s* states the excitons in the k-space ($g_{ij}^{\mathrm{ns}}(\mathrm{k})$). In addition, because of their roles in the PI ISTs, in the following we refer to $I_{1,j}^{\nu}$ and $I_{2,j}^{\nu}$ as dipole moment mixing factors (DMMFs). Note also that despite of some similarities, Eqs. (13)–(15) are different from those presented in Ref. 9. This is because in this reference the fact that only a specific spinor of holes can contribute to the formation of excitons was ignored. As we will show in the following such a treatment can only be valid when one considers the hole dispersions are parabolic.

III. EXCITONIC EFFECTS IN THE PHOTOINDUCED INTERSUBBAND TRANSITIONS

A distinct feature of our treatment in this paper is inclusion of the hole spinor mixing effects in the PI ISTs. To

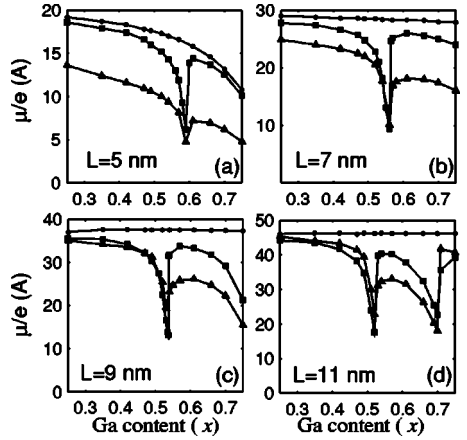

FIG. 2. Normalized dipole moments of the PI-ISTs associated with the transitions between the 1*s* states of the e1-hh1 and e2-hh1 excitons. Squares refer to the PI ISTs associated with nonactive e1-hh1 excitons ($\mu_{\mathrm{hh1}}^{\mathrm{nact}}/e$) and triangles to those associated with excitons that are being optically excited or decaying radiatively ($\mu_{\mathrm{hh1}}^{\mathrm{act}}/e$). The dots refer to the dipole moments associated with the e1-e2 transitions excluding any excitonic effect ($\mu_{12}^{\mathrm{ele}}/e$).

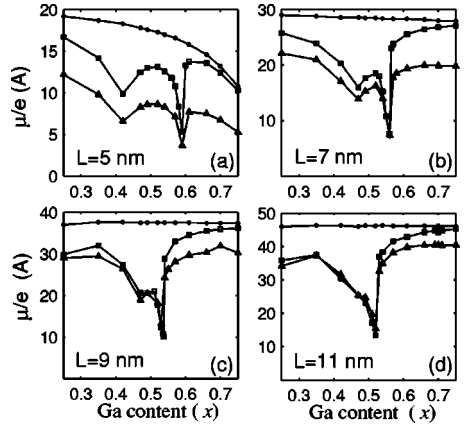

FIG. 3. Normalized dipole moments of the PI-ISTs associated with the transitions between the 1s states of the e1-lh1 and e2-lh1 excitons. Here squares refer to $\mu_{\mathrm{lh1}}^{\mathrm{nact}}/e$, and triangles to $\mu_{\mathrm{lh1}}^{\mathrm{act}}/e$. All other specifications are similar to those in Fig. 2.

investigate these effects and find out how optically active and nonactive excitons can influence these transitions here we consider $In_{1-x}Ga_xAs/InP$ QW structures with various thicknesses. We also study the effects of strains associated with the different values of x on these transitions. To start we first investigate the dipole moments associated with the PI ISTs between the 1*s* states of the e1-hh1 and e2-hh1 excitons. As shown in Fig. 2(a), when $L=5$ nm for the ranges of $x\lesssim 0.45$ and $x\gtrsim 0.6$ the dipole moments of the PI IST associated with the nonactive excitons ($\mu_{\mathrm{hh1}}^{\mathrm{nact}}$, squares) are very similar to μ_{12}^{ele} (dots) but larger than those associated with the active excitons ($\mu_{\mathrm{hh1}}^{\mathrm{act}}$, triangles). This trend changes dramatically at the vicinity of $x\sim 0.57$ (0.7% tensile strain) where $\mu_{\mathrm{hh1}}^{\mathrm{nact}}$ becomes about one third of μ_{12}^{ele}. This process is accompanied by the reduction of $\mu_{\mathrm{hh1}}^{\mathrm{act}}$, allowing it having similar values as those of $\mu_{\mathrm{hh1}}^{\mathrm{nact}}$ at $x\sim 0.57$.

As L increases and $x\lesssim 0.52$ the differences between $\mu_{\mathrm{hh1}}^{\mathrm{nact}}$ and $\mu_{\mathrm{hh1}}^{\mathrm{act}}$ are decreased while they become close to μ_{12}^{ele}. For $x\gtrsim 0.52$, however, $\mu_{\mathrm{hh1}}^{\mathrm{nact}}$ and $\mu_{\mathrm{hh1}}^{\mathrm{act}}$ depart from μ_{12}^{ele} as they vary with x more rapidly [Figs 2(b) and 2(c)]. When $L=11$ nm [Fig. 2(d)], at $x_c\sim 0.7$ (1.6% tensile strain) this process ends up with the generation of another minimum for each of these dipole moments. Here the magnitudes of these dipole moments is less than 50% of μ_{12}^{ele}. For such a thickness, when $x\lesssim 0.51$ we find $\mu_{\mathrm{hh1}}^{\mathrm{nact}}$ and $\mu_{\mathrm{hh1}}^{\mathrm{act}}$ are similar to μ_{12}^{ele}.

Evolutions of the dipole moments associated with the PI ISTs between the 1*s* states of the e1-lh1 and e2-lh1 excitons are also peculiar. Here similar to Fig. 2(a), for $L=5$ nm and $x<0.57$ $\mu_{\mathrm{lh1}}^{\mathrm{act}}$ is less than $\mu_{\mathrm{lh1}}^{\mathrm{nact}}$ although they have similar variation with x [Fig. 3(a)]. In contrast to Fig. 2(a), however, here they are two minima, one at $x\sim 0.42$ and the other at $x\sim 0.57$. As L increases the spacing between these two minima decreases while $\mu_{\mathrm{lh1}}^{\mathrm{nact}}$ and $\mu_{\mathrm{lh1}}^{\mathrm{act}}$ become similar. For $L=11$ nm there is virtually only one minimum at $x\sim 0.52$. Here except for $x>0.52$ these dipole moments are virtually overlapped. Note that a specific feature of the most of the dipole moment dips seen in Figs. 2 and 3 is that they are asymmetric around the x's where the minima occur. These issues and others will be discussed in the following section.

Note that the results presented in Figs. 2 and 3 are valid when the PI ISTs occur between bound exciton states. In addition, the nature of these transitions, in terms of their associations with the active or nonactive excitons, and their relative contributions to the nonlinear optical processes involving PI ISTs mainly depend on the conditions of the QW sample and the experiment. These include intensity and frequency of the IR laser field responsible for these transitions, time delay between this field and the interband laser field generating electron-hole pairs, the type of the physical quantity is measured, and the scattering rates of excitons with phonons, other excitons, disorder, etc. To clarify this let us first consider the case where the bound excitons are generated by near-IR laser pulses resonantly exciting the 1*s* or 2*s* states of the e1-hh1 or e1-lh1 excitons with $K\sim 0$. Here one can only deal with the PI ISTs associated with the active excitons if before these pulses reach the sample the QW structure is influenced by the longer IR laser pulses and when the interband absorption is monitored. In this scheme, which has been used in the past to study optical quantum confined Stark effects,[11,18] and all-optical modulators,[22] the near bandedge exciton peaks are detected while the IR field is strong enough to mix the conduction subbands associated with the PI ISTs (here e1 and e2). As a result, the upper levels of the excitonic interband transitions are renormalized with a scale determined by the dipole moments of the PI ISTs associated with the active excitons. Note that in general the upper transition levels of the PI ISTs (the 1*s* and 2*s* states of the e2-hh1 or e2-lh1 excitons) are scattered with acoustic or longitudinal optical (LO) phonons, depending on the e1-e2 energy spacing. This leads to the ionization of these excitons and formation of the e1-hh1 or e1-lh1 excitons with large K.[12] Therefore, while in the optically accessible region ($K\sim 0$) the IR driven PI ISTs associated with the active excitons determine the evolution of the interband absorption, outside this region the PI ISTs associated with nonactive excitons can occur.

If the IR pulses reach the sample after the near-IR interband field the resonantly excited excitons can be scattered

with phonons, other excitons, disorder, etc., or thermally ionized and then reformed again before the PI ISTs occur. As a result, the momenta of some of the e1-hh1 or e1-lh1 excitons can become so large that the momentum conservation restriction drastically hinders their emission. Here, however, if one studies the effects of an intense IR field resonant with the PI ISTs on the photoluminescence of a QW,[12] only active excitons are involved. In fact here, similar to the case when the interband absorption is monitored, the IR field acts as a pump and the exciton emission (or absorption) as a probe. However, if one uses the IR field as a probe and the near IR field as a pump,[4] then combination of PI ISTs associated with both active and nonactive can be present.

When the near-IR interband field off-resonantly excites the electron-hole pairs, formation of active or nonactive excitons requires more attention. This is because depending on the frequency and intensity of this field and temperature different scenarios can happen. In fact based on a recent microscopic study the near bandedge emission at the 1*s* resonance is not necessarily caused by the radiative decay of exciton population, but rather due to the Coulomb enhanced radiative recombination of the electron-hole pairs.[26] As a result, interaction of an IR laser field resonant with the $e1$-$e2$ transitions with a QW may not be involved with the PI ISTs associated with the exciton states, even if a distinct emission peak appears at the 1*s* resonance. Having this in mind to remain within the exciton population limit, as required in this paper, here one should consider low or intermediate carrier densities with small excess kinetic energies at low temperatures.[27–29] In general, however, in an off-resonantly excited QW the electron-hole pairs first form excitons with large K. These excitons then undergo energy and momentum relaxation until they reach the optically accessible region where they are able to decay radiatively.[30,31] Here to treat the PI ISTs and include the effects of active and nonactive excitons, similar considerations as those in the case of the resonant excitation should be considered.

IV. EXCITONIC INTERBAND TRANSITIONS AND THE PHOTOINDUCED INTERSUBBAND TRANSITIONS

To discuss the results presented in the previous section, note that when an exciton is optically generated or decay radiatively an electron-hole pair is either created or annihilated. These processes require the coordinates of the electron and hole ($\mathbf{r_e}$ and $\mathbf{r_h}$) be the same. For this reason the excitonic interband transitions not only depend on the overlap integral between electron and hole wave functions, but also on $|\Phi_{e1,j}(0)|^2$ [$\Phi_{e1,j}(\mathbf{r_e}-\mathbf{r_h})$ is the Fourier transform of $G_{e1,j}(\mathbf{k})$]. The coordinate requirement stands when the excitonic interband transitions (optical excitation or radiative decay of excitons) are accompanied with the PI ISTs. On the other hand, when excitons are in their nonradiative states or they are not decaying, although the electrons' and holes' coordinates can overlap, such a requirement does not exist.

Having these in mind, as shown in Figs. 2 and 3, one expects that the PI ISTs are influenced differently by the excitonic effects, depending whether the e1-hh1 or e1-lh1 excitons are in their nonradiative states or they are being optically excited or radiatively decaying (active excitons). For those associated with the nonactive excitons, as shown in Eqs. (13)–(15), the excitonic effects mostly come as a normalization factor of the dipole moment associated with the $e1$-$e2$ transitions (μ_{12}^{ele}). For the case of the active excitons, however, the PI IST dipole moments are convoluted with the hole probability at each k [Eq. (10)].

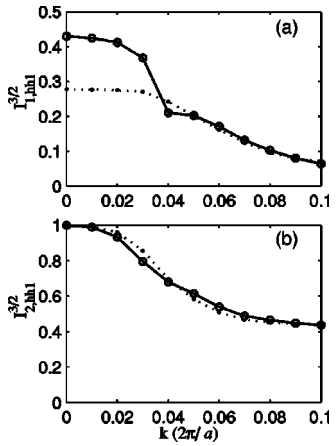

FIG. 4. Dipole moment mixing factors of the e1-hh1 to e2-hh1 PI ISTs associated with active (a) and nonactive excitons (b) for $x=0.25$. Dots refer to $L=5$ nm and circles to $L=11$ nm. a refers to the lattice constant of the $In_{0.75}Ga_{0.25}As$ QW.

To understand how these features influence the PI IST dipole moments, let us consider $\mu_{\mathrm{hh1}}^{\mathrm{act}}$ and $\mu_{\mathrm{hh1}}^{\mathrm{nact}}$ for $L=5$ nm [Fig. 2(a)] and 11 nm [Fig. 2(d)] and $x=0.25$ (1.5% compressive strain). Since the magnitudes of these moments directly depend on $I_{1,\mathrm{hh1}}^{3/2}$ or $I_{2,\mathrm{hh1}}^{3/2}$, it is useful to study evolution of these integrals under these conditions. As shown in Fig. 4, the first distinct difference between $I_{1,\mathrm{hh1}}^{3/2}$ and $I_{2,\mathrm{hh1}}^{3/2}$ is that at $k=0$ the latter always starts from unity [Fig. 4(b)], as required by the fact that hh1 and lh1 contain only $+3/2$ and $-1/2$ spinors at the zone center, respectively. The former, however, is much less than unity and has a relatively strong dependency on L [Fig. 4(a)]. Here as L increases from 5 to 11 nm, while $I_{2,\mathrm{hh1}}^{3/2}$ remains fairly unchanged, within a region close to the zone center $I_{1,\mathrm{hh1}}^{3/2}$ enhances significantly. Since the exciton wave functions are mostly centered in this region, such an enhancement process increases the magnitude of $\mu_{\mathrm{hh1}}^{\mathrm{act}}$, allowing it becoming similar to $\mu_{\mathrm{hh1}}^{\mathrm{nact}}$ and μ_{12}^{ele}.

V. HOLE SPINOR MIXING EFFECTS IN THE PHOTOINDUCED INTERSUBBAND TRANSITIONS

The results presented in Fig. 4 show that, except for a region at the proximity of the zone center, as k increases $I_{j,\mathrm{hh1}}^{\nu}$ are decreased significantly. This can be attributed to the spinor mixing of the hole subbands. Here because of the extensive amount of compressive strain (1.5%) at the vicinity of the zone center hh1 is mainly parabolic, as shown in Fig. 5(a). As a result, the states of hh1 in this region are mainly associated with $\nu=3/2$. For $k \gtrsim 0.02(2\pi/a)$ (a is the lattice constant of the QW), however, the spinor mixing of the hole subbands gradually increases as the hh1 dispersion become increasing nonparabolic. As this happens the states of hh1

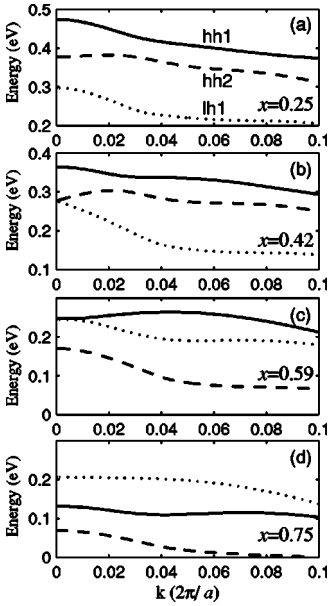

FIG. 5. Band structure of a 5 nm $In_{1-x}Ga_xAs$ QW structure with InP barrier for $x=0.25$ (a), 0.42 (b), 0.59 (c) and 0.75 (d).

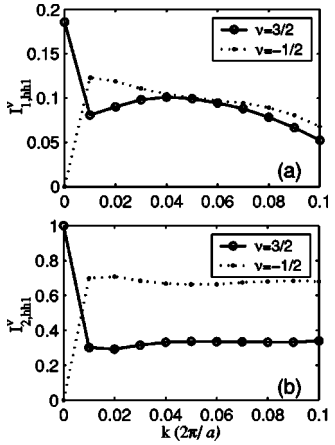

FIG. 6. Dipole moment mixing factors for a 5 nm $In_{0.41}Ga_{0.59}As$ QW structure with InP barrier. (a) refers to the PI ISTs associated with the e1-hh1 excitons that are either optically excited or decaying radiatively and (b) refers to the case where these excitons are nonactive.

becomes a mixture of the $\nu=3/2$ and $\nu=-1/2$ spinors.

Having these in mind, one can find spinor mixing of the hole subbands responsible for the variations of the dipole moments of the PI ISTs with x and explain their deviations from μ_{12}^{ele} (Figs. 2 and 3). To see this note that based on Eqs. (9) and (13) μ_j^{nact} and μ_j^{act} mostly depend on the magnitudes and the k-dependencies of $I_{1,j}^{\nu}$ and $I_{2,j}^{\nu}$ in the effective region of the k-space where the exciton wave functions are centered. For example, in the case of $L=5$ nm and $x=0.25$, as shown in Fig. 4(b) (dots), $I_{2,\text{hh1}}^{\nu}$ depends weakly on k in this region while its magnitude is close to unity. Combining this with the fact that under such conditions the normalization condition of the exciton wavefunctions [Eq. (13)] is well utilized, one can explain why for $x<0.4$ $\mu_{\text{hh1}}^{\text{nact}}$ is similar to μ_{12}^{ele} [Fig. 2(a)]. Similarly, the results in Fig. 4(b) also explain why for $L=11$ nm and $x=0.25$ (circles) $\mu_{\text{hh1}}^{\text{nact}}$ and μ_{12}^{ele} are nearly the same. As shown in Fig. 4(a), however, the case of the active excitons can be different. Here, in contrast to the case of nonactive excitons, for $L=11$ nm the magnitude of $I_{1,\text{hh1}}^{3/2}$ for $x=0.25$ in the effective region of the excitons is larger than that of $L=5$ nm. This explains why for $x<0.4$ and $L=5$ nm $\mu_{\text{hh1}}^{\text{act}}$ is less than μ_{12}^{ele} but when L is increased to 11 nm they become similar.

As strain or Ga content (x) changes or/and the QW becomes thicker, the contributions of $\nu=3/2$ and $-1/2$ in hh1 and lh1 are changed. This is translated into the distinct features seen in Figs. 2 and 3, including creation of the minima in μ_j^{act} and μ_j^{nact}. To explain these issues note that as the thickness of the QW increases the energies of the hole subbands are changed, allowing them to get closer to each other. In addition, as x increases from 0.25 to 0.75 the QW structure strain is changed from 1.5% compressive to 1.95% tensile. Figure 5 shows the effects of the latter on the dispersions of hh1 (solid line), hh2 (dashed line), and lh1 (dotted line) for $L=5$ nm. Note that as x increases these subbands can become degenerate in some regions of k-space with strongly nonparabolic dispersions, or obtain parabolic dispersions while are isolated from others. Using these features we can explain the results presented in Figs. 2(a) and 3(a). We start with the minimum seen in Fig. 2(a) at $x=0.59$ (0.84% tensile strain). As seen in Fig. 5(c), under such a condition hh2 is pushed down while hh1 becomes strongly nonparabolic and nearly degenerate with lh1 around the zone center. In fact here with a slight more increase of x these two subbands are crossed over and lh1 becomes the first hole subband. This phenomenon leads to a strong spinor mixing and suppresses the contributions of $\nu=3/2$ in hh1 and $\nu=-1/2$ in lh1. This is accompanied with the increase of the contributions of $\nu=-1/2$ and $+3/2$ in these subbands, respectively. To see this in Fig. 6 we show the DMMFs associated with active ($I_{1,\text{hh1}}^{3/2}$) and nonactive heavy-hole excitons ($I_{2,\text{hh1}}^{3/2}$) for $L=5$ nm and $x=0.59$. Here, in contrast to that seen in Fig. 4, $I_{1,\text{hh1}}^{3/2}$ and $I_{2,\text{hh1}}^{3/2}$ (circles) are changed rapidly around the zone center. As shown in Eqs. (9) and (13), such a feature suppresses the normalization factor of the 1s-states of the excitons and reduces the contribution of the DMMFs in the effective region of the k-space, causing a drastic decrease of $\mu_{\text{hh1}}^{\text{act}}$ and $\mu_{\text{hh1}}^{\text{nact}}$ [Fig. 2(a)]. Note that in Fig. 6 we also show the variation of $I_{1,\text{hh1}}^{-1/2}$ and $I_{2,\text{hh1}}^{-1/2}$ for the sake of completeness and clarity. These DMMFs do not play any role in the PI ISTs discussed in this paper.

Note that around the crossover point shown in Fig. 5(c) the strong mixing of hh1 is accompanied with the strong mixing of lh1. As shown in Fig. 3(a), this leads to the minima seen in $\mu_{\text{lh1}}^{\text{act}}$ and $\mu_{\text{lh1}}^{\text{nact}}$ at $x\sim0.59$—the same x as that of hh1 in Fig. 2(a). In the case of lh1, however, for each of these dipole moments an extra minimum at $x\sim0.42$ has occurred. One can use the hh2 and lh1 dispersions seen in Fig. 5(b) to explain this feature. When $x\sim0.42$ these two subbands are about to cross over. This leads to a cetain amount of mixing for lh1 around the zone center causing the minima seen at $x\sim0.42$. Note that the asymmetry seen in the minima in Figs. 2 and 3 can be attributed to the fact that as lh1 reaches hh1 mixing of $\nu=3/2$ and $\nu=-1/2$ spinors in both

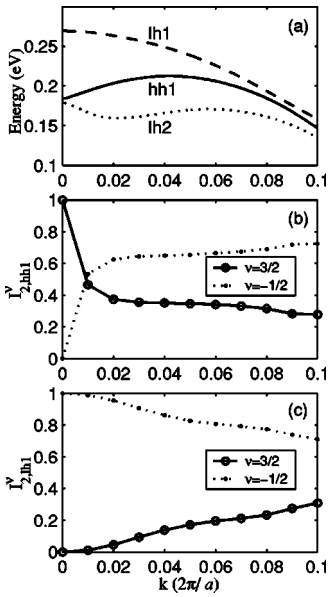

FIG. 7. (a) Band structure of a 11 nm $In_{0.3}Ga_{0.7}As$ QW structure with InP barrier. (b) and (c) refer, respectively, to $I^{\nu}_{2,hh1}$ and $I^{\nu}_{2,lh1}$.

hh1 and lh1 increases. However, right after the crossover the contributions of $\nu=3/2$ in hh1 and $\nu=-1/2$ in lh1 become increasingly dominant, as mixing reduces drastically.[32] Note that as shown in Fig. 5(d), for $x=0.75$ this leads to a very parabolic dispersion for lh1. This explains the sharp increase of $\mu^{\text{nact}}_{\text{lh1}}$ and its similarity with μ^{ele}_{12} when the structure is under extensive amount of tensile strain.

Similar concepts can also be used to explain other results presented in this paper, including generation of the two minima in Fig. 2(d) and evolutions of those in Fig. 3 as QW thickness increases. To see this note that, as mentioned above, the crossover of hh2 and lh1 at $x\sim0.42$ and that of hh1 and lh1 at $x\sim0.59$ were responsible for the generation of two minima seen in Fig. 3(a). As L increases, however, the hole subbands are energetically become closer to each other and, therefore, the x's where these crossovers happen become closer to each other. Therefore, with a slight increase of x one can go from one minimum to another. For $L=11$ nm this leads to a nearly single peak for $\mu^{\text{act}}_{\text{lh1}}$ and $\mu^{\text{nact}}_{\text{lh1}}$ at $x\sim0.52$ [Fig. 3(d)]. For the same QW thickness, however, $\mu^{\text{act}}_{\text{hh1}}$ and $\mu^{\text{nact}}_{\text{hh1}}$ have an extra minimum at $x\sim0.7$ [Fig. 2(d)]. To explain this we show in Fig. 7 the hole dispersions and the DMMFs associated with $\mu^{\text{nact}}_{\text{hh1}}$ [Fig. 7(b), circles] and $\mu^{\text{nact}}_{\text{lh1}}$ [Fig. 7(c), dots] when $L=11$ nm and $x=0.7$. Here one can see that lh1 is very much parabolic (dashed line) causing $I^{-1/2}_{2,\text{lh1}}$ changes slowly with k [Fig. 7(c)]. On other hand, however, under the same conditions hh1 has become increasingly nonparabolic [Fig. 7(a), solid line]. This makes $I^{3/2}_{2,\text{hh1}}$ strongly k-dependent [Fig. 7(b)] and reduces the dipole moments associated with the transitions between 1s states of e1-hh1 and e2-hh1.

The results obtained in this paper suggest that even in a structure that contains no strain, the effects of hole spinor mixing and excitonic interband transitions in the PI ISTs can be significant. For the $In_{1-x}Ga_xAs/InP$ QW structures considered in this paper the zero strain case occurs when $x\sim0.47$. Under this condition, due to the nonparabolic dispersion of the lh1 subband $\mu^{\text{nact}}_{\text{lh1}}$ is much less than μ^{ele}_{12} [Fig. 3(a)]. $\mu^{\text{act}}_{\text{lh1}}$, however, is suppressed more since in addition to the hole mixing effect it is influenced by the excitonic interband transitions. In the case of PI ISTs associated with hh1, depending on the QW thickness, the zero-strain structure can have different contribution from the hole spinor mixing. For narrow QWs, when $x\sim0.47$ hh1 is mainly parabolic and $\mu^{\text{nact}}_{\text{hh1}}$ is close to μ^{ele}_{12}. As the QW thickness increases, hh1 can become more nonparabolic causing more suppression. Here, however, the most significant deviation of the PI IST dipole moments from μ^{ele}_{12} occurs in narrow QWs when these transitions are accompanied with the excitonic interband transitions [Fig. 2(a)].

VI. CONCLUSIONS

In conclusion, we studied the effects of hole subband spinor mixing and the excitonic interband transitions in the photoinduced conduction intersubband transitions. We showed that when such intersubband transitions were accompanied with the interband transitions, such as optical excitation or radiative decay of excitons, their dipole moments could be suppressed drastically. We attributed such a suppression to the correlation between the photo-excited electron and hole coordinates when an electron-hole pair is generated or annihilated. We also showed that when hole subbands were strongly nonparabolic the dipole moments associated with the PI ISTs were much smaller than those obtained considering only electron wavefunctions. This effect become particularly significant when due to strain the hole subbands are about to cross over each other.

ACKNOWLEDGMENTS

This research was supported by the Natural Sciences and Engineering Research Council of Canada and Photonic Research Ontario.

*Present address: Photonami, Inc., 50 Mural Street, Richmond Hill, Ontario, Canada L4B 1E4. Electronic address: sm.sadeghi@utoronto.ca

[1] F. H. Julien, P. Vagos, J.-M. Lourtioz, D. Yang, and R. Planel, Appl. Phys. Lett. **59**, 2645 (1991).

[2] B. F. Levine, J. Appl. Phys. **74**, R1 (1993).

[3] C. Gmachl, F. Capasso, D. L. Sivco, and A. Y. Cho, Rep. Prog. Phys. **64**, 1533 (2001).

[4] R. Duer, I. Shtrichman, D. Gershoni, and E. Ehrenfreund, Phys. Rev. Lett. **78**, 3919 (1997).

[5] R. Duer, D. Gershoni, and E. Ehrenfreund, Superlattices Microstruct. **17**, 5 (1995).

[6] S. Sauvage, P. Baucaud, F. Julien, J.-M. Gerard, and J.-Y. Marzin, J. Appl. Phys. **82**, 3396 (1997).
[7] S. Calderon, O. Kadar, and A. Sa'ar, Phys. Rev. B **62**, 9935 (2000).
[8] M. Olszakier, E. Ehrenfreund, E. Cohen, J. Bajaj, and G. Sullivan, Phys. Rev. Lett. **62**, 2997 (1989).
[9] W. J. Li, B. D. McCombe, F. A. Chambers, G. P. Devane, J. Ralston, and G. Wicks, Phys. Rev. B **42**, 11953 (1990).
[10] S. M. Sadeghi and W. Li, IEEE J. Quantum Electron. **40**, 343 (2004).
[11] D. Frohlich, R. Wille, W. Schlapp, and G. Weimann, Phys. Rev. Lett. **59**, 1748 (1987).
[12] S. M. Sadeghi and J. Meyer, J. Phys.: Condens. Matter **12**, 5801 (2000).
[13] J. Christen and D. Bimberg, Phys. Rev. B **42**, 7213 (1990).
[14] R. Schnabel, R. Zimmermann, D. Bimberg, H. Nickel, R. Losch, and W. Schlapp, Phys. Rev. B **46**, 9873 (1992).
[15] V. Negoita, D. Snoke, and K. Eberl, Phys. Rev. B **60**, 2661 (1999).
[16] I. Shtrichman, A. Ron, D. Gershoni, E. Ehrenfreund, K. Maranowski, and A. Gossard, Phys. Rev. B **65**, 153302 (2002).
[17] T. Muller, W. Parz, G. Strasser, and K. Unterrainer, Appl. Phys. Lett. **84**, 64 (2004).
[18] D. Frohlich, C. Neumann, S. Spitzer, and R. Zimmermann, in *Optics of Excitons in Confined Systems, Giardini Naxos*, edited by A. D. Andrea, R. D. Sole, R. Girlanda, and A. Quatropani (Inst. Phys., 1991), Vol. 123, p. 227.
[19] M. Su, S. Carter, M. Sherwin, A. Huntington, and L. Coldren, Phys. Rev. B **67**, 125307 (2003).
[20] A. Moslov and D. Citrin, Phys. Rev. B **64**, 155309 (2001).
[21] A. Neogi, H. Yoshida, T. Mozume, and O. Wada, Opt. Commun. **159**, 225 (1999).
[22] S. Noda, M. Ohya, T. Sakamoto, and A. Sasaki, IEEE J. Quantum Electron. **32**, 448 (1996).
[23] L. C. Andreani and A. Pasquarello, Phys. Rev. B **42**, 8928 (1990).
[24] B. Zhu and K. Huang, Phys. Rev. B **36**, 8102 (1987).
[25] R. Winkler, Phys. Rev. B **51**, 14395 (1995).
[26] M. Kira, F. Jahnke, and S. W. Koch, Phys. Rev. Lett. **81**, 3263 (1998).
[27] D. Hagele, J. Hubner, W. W. Ruhle, and M. Oestreich, Physica B **271**, 328 (1999).
[28] W. Hoyer, M. Kira, and S. Koch, Phys. Rev. B **67**, 155113 (2003).
[29] S. Chatterjee, C. Ell, S. Mosor, G. Khitrova, H. Gibbs, W. Hoyer, M. Kira, S. Koch, J. Prineas, and H. Stolz, Phys. Rev. Lett. **92**, 067402 (2004).
[30] T. Damen, J. Shah, D. Oberli, D. Chemla, J. Cunningham, and J. Kuo, Phys. Rev. B **42**, 7434 (1990).
[31] R. Kaindl, M. Carnahan, D. Hagele, R. Lovenich, and D. Chemla, Nature (London) **423**, 734 (2003).
[32] T. Hiroshima, Phys. Rev. B **36**, 4518 (1987).